Disordered electrical potential observed on the surface of SiO_2 by electric field microscopy

2010 J. Phys.: Condens. Matter 22 045002

(http://iopscience.iop.org/0953-8984/22/4/045002)

J. Phys.: Condens. Matter **22** (2010) 045002 (6pp) doi:10.1088/0953-8984/22/4/045002

Disordered electrical potential observed on the surface of SiO_2 by electric field microscopy

N García[1,2], Zang Yan[1], A Ballestar[1], J Barzola-Quiquia[2], F Bern[2] and P Esquinazi[2]

[1] Laboratorio de Física de Sistemas Pequeños y Nanotecnología, Consejo Superior de Investigaciones Científicas, E-28006 Madrid, Spain
[2] Division of Superconductivity and Magnetism, Institut für Experimentelle Physik II, Universität Leipzig, Linnéstraße 5, D-04103 Leipzig, Germany

E-mail: esquin@physik.uni-leipzig.de

Received 16 October 2009, in final form 8 December 2009
Published 5 January 2010
Online at stacks.iop.org/JPhysCM/22/045002

Abstract
The electrical potential on the surface of ∼300 nm thick SiO_2 grown on single-crystalline Si substrates has been characterized at ambient conditions using electric field microscopy. Our results show an inhomogeneous potential distribution with fluctuations up to ∼0.4 V within regions of 1 μm. The potential fluctuations observed at the surface of these usual dielectric holders of graphene sheets should induce strong variations in the graphene charge densities and provide a simple explanation for some of the anomalous behaviors of the transport properties of graphene.

(Some figures in this article are in colour only in the electronic version)

1. Introduction

Nowadays, the study of graphene, i.e. a monolayer of graphite, represents an important research field in physics and material science. Although studies of monolayers of graphite grown on different transitional metal carbides were originally published nearly 20 years ago [1, 2], the simple preparation of these monolayers by exfoliation [3], as well as grown on SiC substrates [4], and their transport properties with the field effect dependence substantially increased the attention of the solid state community. One of the highlighted effects is the electric-field-induced metal–insulator–semiconductor transition that populates the bands of graphene with holes or electrons, bands that have been claimed to be Dirac-like, i.e. following a linear dispersion relation $E \propto |k|$. Also, the observation of quantum Hall effects and the quantization of the conductance has been claimed [5]. The published results in the literature suggest that with this material one may achieve the basis for new nanodevices if, among other details, one could find a way to produce homogeneous, uniform layers [6].

There are, however, some experimental facts indicating that the transport behavior in graphene is far from being ideal. For example, the carrier mobility in samples on dielectric substrates including SiO_2 is of the order of 1 $m^2\ V^{-1}\ s^{-1}$, a value that remains rather independent of the dielectric substrate, temperature and density of carriers, see, e.g., [7] and references therein. On the other hand, if the experiments are done with suspended graphene samples, i.e. without touching the substrate, the mobility drastically increased [8, 9]. The experimental data suggest that one of the main problems of graphene on dielectric substrates could come from the substrate's non-uniform electrical potential.

As nearly perfect insulators, we expect that oxides do not exhibit a uniform potential distribution just because of the existence of a distribution of charges in their near-surface region, letting a metastable potential distribution develop on it. In this case the deposited graphene will be strongly affected by the same variations of potential the dielectric substrate has. It is interesting to note the results of an experimental study using a scanning single-electron transistor that observed puddles of electrons and holes on the graphene surface [10]. The obtained images reveal a rather disordered domain-like array of fluctuating potential, which might be due to the substrate influence and not intrinsic

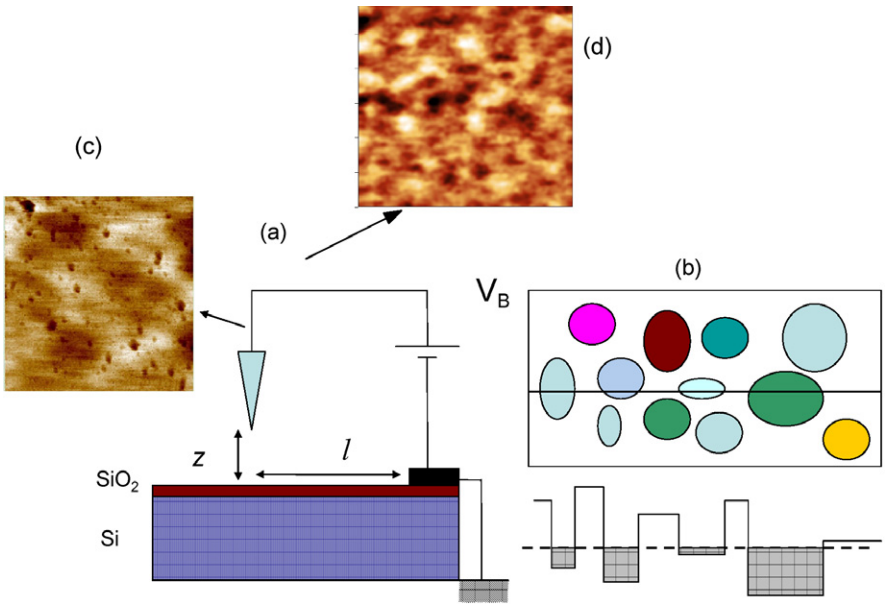

Figure 1. (a) Sketch of the experimental arrangement. The distance z between tip and surface can be changed as well as the distance l to the mass contact. (b) Sketch of the potential distribution for which a graphene layer would be affected if it is attached to the surface. The scan line below represents a one-dimensional potential with differently filled wells of graphene carriers. For simplicity only electron-filled bands are depicted. The dashed line represents the Fermi energy of the graphene layer on top of the disordered potential surface. (c) EFM picture (4×4 μm^2) of an SiO_2 surface in a sample in which a resin rest (dark spots) was left. (d) EFM picture (6×6 μm^2) of a resin-free sample. These results were obtained with two different microscopes and different EFM tips. For both EFM pictures the potential gradients between light and dark broad areas (not spots) are $\leqslant$0.4 V.

to graphene. A simple estimate should clarify for the reader the electrical potential fluctuations we may expect. In general, a voltage difference of ∼10 V between graphene and the ∼300 nm thick SiO_2 layer is necessary to produce a clear change in its carrier density when the resistance shows a maximum, i.e. around the 'neutrality-' (former Dirac-) point. This means an electric field of the order of 3×10^7 V m^{-1}. A potential fluctuation of ∼0.1 V coming from charges distributed at random within a thickness of ∼10 nm in the dielectric layer would produce a similar electric field. Therefore, it will generate a change in the carrier density and in the overall potential distribution, affecting the transport of the carriers within the 2D graphene layer.

Further indirect evidence for the potential influence of the substrate comes from the fact that in transport experiments done in graphene samples one needs to apply a magnetic field to increase the sample conductivity, arguing that otherwise the carriers are localized [11]. In this work we argue that several of these observations and effects are due to the influence of the dielectric substrate potential at its near-surface region. Because of the previous arguments we would like to use electric field microscopy (EFM) to analyze the surface of the SiO_2 and try to see if we have potential fluctuations and measure their magnitude. This will tell us what is the initial state of the potential the graphene sees before shifting the electron and hole bands via a bias voltage.

2. Model and method

Consider an EFM arrangement shown schematically in figure 1(a) where a potential U_{tip} is applied between the metal tip and the surface of the oxide sample. The potential difference between tip and surface will be neither zero nor constant at the surface of SiO_2. The applied electric field will penetrate into the oxide a certain penetration depth λ that depends on the total screening characteristics of the material. Due to the vanishingly low carrier density of SiO_2 it is expected that the electric field penetration depth $\lambda \propto 1/(n^{1/6}\sqrt{m^\star})$ ($m^\star$ is the effective mass) would be >10 nm for carrier density $n < 10^{14}$ cm^{-3}. Note that there is a large electrical resistance between the point of the surface where the tip is and the contact to the mass. Therefore the bias voltage applied V_B is between the tip and the thick oxide layer and the potential drop between the sample tip position and the contact on the surface to the mass (distance l in figure 1(a)). Notice, however, that the last potential drop will be constant in all the measurements because the scan we perform is of the order of 5×5 μm^2 and the distance from the tip position to the contact is $l > 0.1$ mm.

The samples we used are the usual p-type, polished Si substrates (100) (Crystec, Germany) with resistivity $\rho \sim 0.02$ Ω cm and $a \simeq 300$ nm thick amorphous SiO_2 at the surface grown by thermal annealing. Some of the substrates were covered by a layer of insulating optical resin (Pietlow Brandt GmbH, Germany) that was partially removed with ethanol in some of the samples to investigate the influence of resin rest on the EFM signal. Other Si substrates without resin coverage were also measured. The measurements at ambient conditions were done with two EFM microscopes: an AFM from NTI Solver and a Dimension 3000 with Extender Electronics Module from Veeco. The results presented in this work were obtained using the EFM mode in both. Kelvin force microscopy (KFM) was also used with similar results.

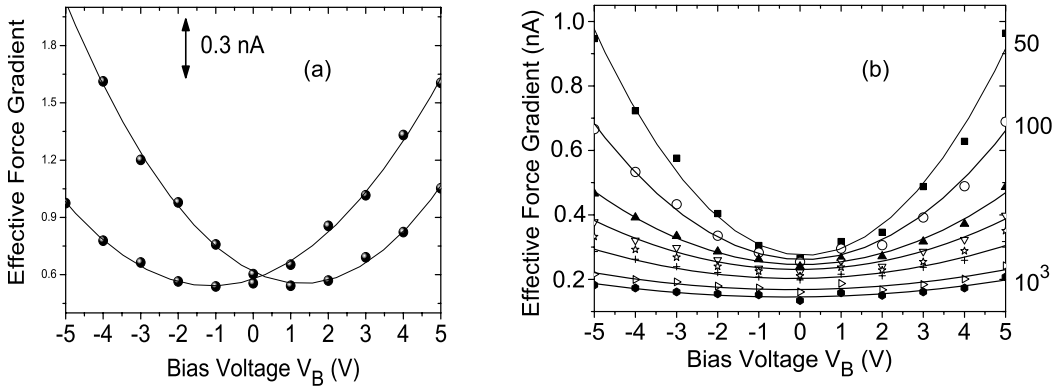

Figure 2. Effective force gradient in nA versus bias voltage $V_B \propto U_{tip}$. (a) Two curves obtained at a height of 100 nm between the tip and surface at two different positions on the sample. (b) The same but at different heights at a position of the sample where the minima is at $V_B \simeq 0$ V. The intermediate curves were taken at heights of 200, 300, 400, 500 and 800 nm. All the continuous lines are simple quadratic fits to the data, in agreement with equation (1).

However, the software for this last method was less suitable for these studies.

Two different conductive cantilevers were used: Olympus OMCL-AC240T M-B2, Pt-coated and W2C-coated tips with resonance frequencies around 150.1 and 76.3 kHz. The measurements were performed in the tapping/lift™ two-pass mode, measuring first the topography and then the frequency shift of the cantilever due to the electrostatic force between the tip and surface. At the first tapping mode no voltage is applied to the tip. If we apply a constant voltage to the tip and scan the sample surface at a constant distance from the sample following the track obtained in the first pass, the measured signal indicates the potential fluctuations on the sample. In the experiment the frequency shift from resonance depends linearly on the force gradient given by [12, 13]

$$\frac{\partial F_z}{\partial z} = \frac{1}{2}\frac{\partial^2 C}{\partial z^2}[U_{tip} - \Psi(x, y)]^2, \tag{1}$$

where U_{tip} is the voltage difference applied between the tip of the cantilever and the surface and $\Psi(x, y)$ is the electrical potential that interacts with the cantilever tip, C is the capacity defined between the tip and surface, see also equation (2). It depends on $\phi(x, y)$, the potential due to charge distribution on the sample near-surface region, and V_{cp}, the difference of work functions between the tip and surface. Within a simple picture one tends to write $\Psi(x, y) = V_{cp} + \phi(x, y)$: however, both terms are interrelated since differences in charge at the surface would imply also a change in work function. Because the exact value of U_{tip} is not known due to the further potential drop within the sample, our results are plotted as a function of the bias voltage $V_B \propto U_{tip}$ that we applied. In the experiments we obtain an effective force gradient signal in nanoampere (nA) units, which is proportional to the force gradient given in equation (1). As explained in [13], taking the proportionality between these signals (or their square root) and V_B, a calibration is done. This calibration is used to transform the measured signals (in nA units) to voltage potential changes. In this way any further calibration in terms of the real force gradient is unnecessary. The measured fluctuations of the potential on the sample surface are transformed in this way from nA to volts, see the bottom picture in figure 5.

3. Results and discussion

Figure 2 shows the measured signals versus V_B at different positions of the SiO_2 surface and at different distances z. The result of having the minima of the signal out of zero, see figure 2(a), is not always observed because of the potential fluctuations. There are other points where the potential falls around zero, as we show in figure 2(b). In this case the effective force gradient signal between -5 and 5 V and for tip heights between 50 and 1000 nm is shown. We observe that all the curves are centered at 0 ± 0.15 V and the curves are practically symmetric with maximum values for 50 nm and minimum for 1000 nm. The amplitude of vibration of the cantilever is ~30 nm and then for $z = 50$ nm the signal depends partially on this vibration. For $z = 1000$ nm the signal is independent of the usual vibration amplitudes but with a relatively large noise-to-signal ratio. The best performances are obtained for 100 nm $\leqslant z \leqslant$ 300 nm. The results below were obtained for $z \simeq 200$ nm. The results presented in figure 2 validate the quadratic dependence given by equation (1). The EFM results presented below are therefore obtained at constant distance z and bias voltage V_B and all the changes in the effective force gradient we measure are due to changes in the function $\Psi(x, y)$.

We have to verify now that the capacitor model describes the experiments. Consider the prefactor of equation (1). If we have a capacitor defined between the tip and surface, then [14]

$$\frac{\partial^2 C}{\partial z^2} = \frac{A}{(z + \lambda)^b}, \tag{2}$$

where A is a geometry factor that depends on the characteristics of the tip–surface arrangement as well as on the applied bias voltage. In the denominator we have the variation with distance tip–surface z and λ is an effective penetration depth of the electric field in the SiO_2. Note that for a metal λ is practically zero but this is not so for an insulator, as shown by

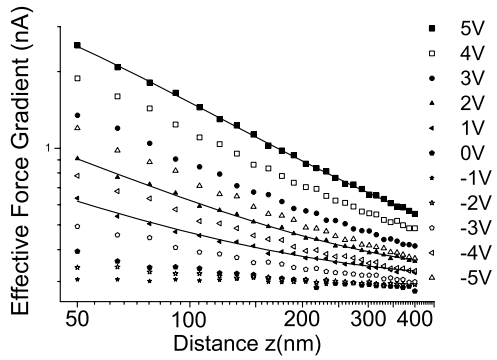

Figure 3. Effective force gradient in nA versus distance between the tip and surface in nm taken at different constant applied voltages (see the right list) in a 'bright' region (see, e.g., figure 1 or figure 4). The continuous lines are fits to the function given by equation (2) with the parameters $A = 380, 100, 56$ nA nm$^{1.2}$ (for the upper, middle and lower curves), $\lambda = 25 \pm 4$ nm and $b = 1.2$ for the three curves.

the results presented in figure 3 where the EFM signal versus distance at constant V_B is plotted. If our system has a deviation from planar electrodes the exponent b in equation (2) should be smaller than 3. This is what we observe from fitting the results in figure 3 obtaining $b = 1.2 \pm 0.04$ and $\lambda = 25 \pm 4$ nm for a region with higher carrier concentration (bright spot) and $\lambda = 35 \pm 9$ nm for a region with lower carrier concentration (dark spot), as expected. The dark regions have less charge and the field should penetrate more.

We now proceed to take topographical data with AFM and then on the same scan line EFM data to see the potential variations with respect to the AFM using the calibration mentioned above. Figure 4 shows the AFM (left) and EFM (right) pictures taken on a different substrate from that shown in figures 1(c) and (d) (we have taken more than 50 scans of this kind on six substrates and all look the same). The white spots correspond to the resin rest that we left to demonstrate that this rest is not the cause of the relatively broad variation of the surface potential and it does not prevent our measuring the topography and potential fluctuations. Similar results are obtained from a sample without any resin rest, see figure 1(d).

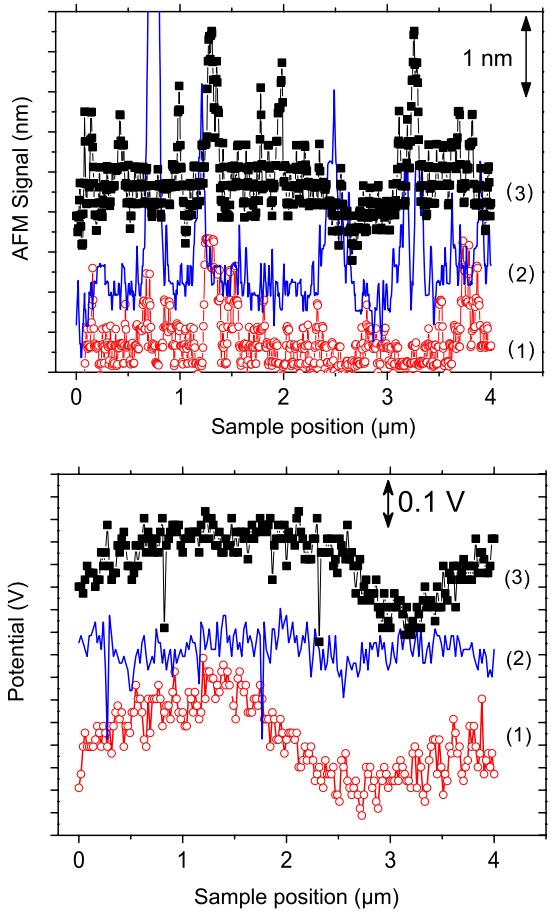

Figure 5. Upper: the picture shows the AFM signals at the three scan lines (1)–(3) shown in figure 4. Bottom: the picture shows the potential versus sample position at the three scan lines shown in the right picture of figure 4. Note that the white spots in the AFM picture correspond to little resin rests that practically do not produce significant changes in the EFM signal, with the exception of the large ones such as the one at the right upper corner.

The pictures in figure 5 show the scans through lines (1)–(3) shown in figure 4. We observe large fluctuations in white and black regions through the entire sample. It is clear from

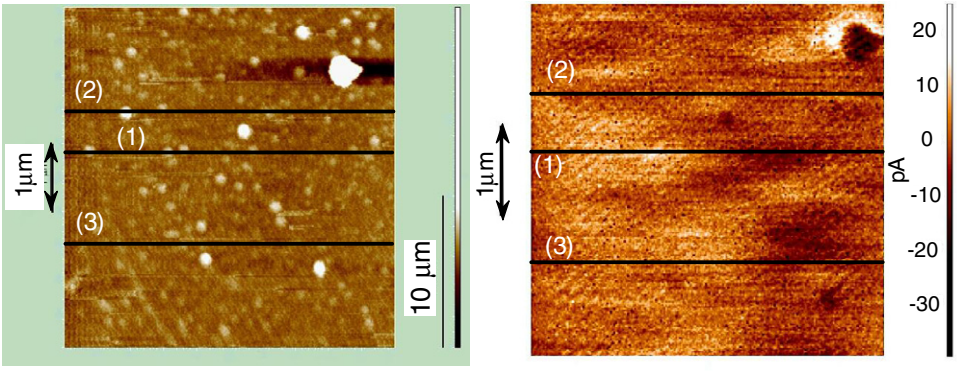

Figure 4. Left: AFM pictures of the SiO_2 surface in a 5×5 μm^2 area (the left bar indicates 1 μm). The pictures below show the AFM signal at the three scan lines (1)–(3). Right: the corresponding EFM result on an area of 3.8×3.8 μm^2 inside the area of (a) obtained at $z = 200$ nm and $V_B = 3$ V. The lower picture shows the potential versus sample position at the three scan lines. Note that the white spots in the AFM picture correspond to little resin rests that practically do not produce significant changes in the EFM signal with the exception of the large ones such as the one at the right upper corner.

the EFM figures that the oxide surface shows relatively large potential fluctuations within microns between 0.1 and 0.3 V for that sample. If these potential fluctuations come from charges within a thickness in the dielectric layer of $\sim 3 \cdots 20$ nm, they will produce electrical field fluctuations of the order of 10^7 V m^{-1}, i.e. comparable to the electric fields used to produce a clear change in the measured resistance or carrier density in graphene. Note that the effect of these potential fluctuations is larger the smaller the carrier density, i.e. the effects are more relevant when the graphene sample is near the neutrality point with a small carrier density.

How much electric charge within the dielectric layer would be necessary to produce such potential fluctuations? Following a similar treatment as in [15] the measured potentials can be produced by a charge density equivalent to $\sim 10^2$ electrons μm^{-3}. Note that, in certain regions, one can also observe potential fluctuations within a distance of 0.1–0.2 μm.

Note that topographic changes in AFM do not influence the EFM signal. All the curves obtained between 100 and 600 nm show the same potential variations because these do not change with the applied voltage, indicating that the topography measurement in the tapping mode scan is reliable. We checked that all measured EFM signals provide the complementary contrast by reversing the voltage polarity applied at the tip, indicating that those signals are due to potential variations and not due to capacitance artifacts, as explained in detail in [13].

The overall EFM results (figures 1 and 4) mean that a graphene layer located on these surfaces will feel directly the potential fluctuations producing regions with higher density of carriers (electrons as well as holes) at the minima (or maxima) and extended regions with a smaller carrier density. In this case the carriers can be partially localized, see the sketch in figure 1(b), and there will be no conductance unless one applies a large enough magnetic field or bias voltage, as observed experimentally [11]. The influence of these potential fluctuations on dielectric substrates may also explain the observation of the quantum Hall effect (QHE), which is apparently not observed for graphene layers with smaller fluctuations or 'better' quality. We note also that, whereas clear signs of the QHE are observed in macroscopic HOPG samples [16, 17], it appears to be absent in mesoscopic multigraphene samples of good quality. This observation appears to be related to the very low amount of carriers that good quality multigraphene samples have [18].

Another aspect is that the so-called Dirac point—claimed to have been reached by some experimentalists in their experiments [5]—has not been actually reached. The carrier density at the Dirac point is several orders of magnitude smaller than the apparently reached minimum of $\sim 10^{10}$ cm^{-2}. Note also that a graphene sample on such a disordered potential distribution indicates that the use of a bias voltage on the transport properties does not ensure at all a Dirac point crossing through the sample. We note that, although a linear dispersion relation for carriers is observed in different spectroscopic experiments, the existence of a Dirac point at sufficiently low energies has not yet been experimentally proved for graphene/graphite. Another point is that the number of carriers is difficult to determine because in real graphene samples and due to the influence of the substrate and/or attached borders for suspended samples there will be regions with many, and regions without, carriers at low enough temperatures, see figure 1(b). We would like to remark that our EFM results have ~ 0.05 μm resolution. At smaller distances there could be additional charge distributions that can also have a strong influence on the carrier mobility of the graphene carriers. The inhomogeneous potential distribution found here on a dielectric substrate provides a simple way to understand the experimentally observed constancy of the carrier mobility on dielectric substrates [7].

4. Conclusion

In conclusion, EFM measurements on SiO_2 surfaces reveal a disordered potential structure of hills and valleys similar to those observed using a single-electron transistor on graphene [10], which are due to intrinsic fluctuations of the dielectric substrate. The potential variations can reach hundreds of mV and therefore the carriers of graphene attached on a dielectric substrate will have difficulties in moving through the sample, affecting their mobility. These results may explain several unclear behaviors reported in the literature on this topic.

Acknowledgments

We gratefully acknowledge the support of the German Science Foundation under DFG ES 86/16-1, the DAAD under grant no. D/07/13369 ('Acciones Integradas Hispano-Alemanas') and the Spanish DGICyT. One of us (NG) was supported by the Leibniz Professor Fellowship of the University of Leipzig.

References

[1] Aizawa T, Souda R, Otani S, Ishzawa Y and Oshima C 1990 *Phys. Rev. Lett.* **64** 768
[2] Itoh H, Ichinose T, Oshima C and Ichinokawa T 1991 *Surf. Sci. Lett.* **254** L437
[3] Novoselov K S, Geim A K, Morozov S V, Dubonos S V, Zhang Y and Jiang D 2004 *Science* **306** 666
[4] Berger C *et al* 2004 *J. Phys. Chem.* B **108** 19912
[5] Geim A K and Novoselov S 2007 *Nat. Mater.* **6** 183 and references therein
[6] Orlita M *et al* 2008 *Phys. Rev. Lett.* **101** 267601
[7] Ponomarenko L A, Yang R, Mohiuddin T M, Katsnelson M I, Novoselov K S, Morozov S V, Zhukov A A, Schedin F, Hill E W and Geim A K 2009 *Phys. Rev. Lett.* **102** 206603
[8] Bolotin K I, Sikes K J, Jiang Z, Klima M, Fudenberg G, Hone J, Kim P and Stormer H L 2008 *Solid State Commun.* **146** 351
[9] Du X, Skachko I, Barker A and Andrei E Y 2008 *Nat. Nanotechnol.* **3** 491
[10] Martin J, Akerman N, Ulbricht G, Lohmann T, Smet J H, von Klitzing K and Yacoby A 2008 *Nat. Phys.* **4** 144
[11] Morozov S V, Novoselov K S, Katsnelson M I, Schedin F, Elias D C, Jaszczak J A and Geim1 A K 2008 *Phys. Rev. Lett.* **100** 016602
[12] Nonnenmacher N, Boyle M O and Wickramasinghe H 1991 *Appl. Phys. Lett.* **58** 2921

[13] Lu Y, Muñoz M, Steplecaru C S, Hao C, Bai M, García N, Schindler K and Esquinazi P 2006 *Phys. Rev. Lett.* **97** 076805
see also the comment by Sadewasser S and Glatzel Th 2007 *Phys. Rev. Lett.* **98** 269701
and the reply by Lu Y *et al* 2007 *Phys. Rev. Lett.* **98** 269702
Proksch R 2006 *Appl. Phys. Lett.* **89** 113121
[14] Naitou Y, Yasaka A and Ookubo N 2009 *J. Appl. Phys.* **105** 044311
[15] Schindler K, García N, Esquinazi P and Ohldag H 2008 *Phys. Rev.* B **78** 045433
[16] Kopelevich Y, Torres J H S, da Silva R R, Mrowka F, Kempa H and Esquinazi P 2003 *Phys. Rev. Lett.* **90** 156402
[17] Kempa H, Esquinazi P and Kopelevich Y 2006 *Solid State Commun.* **138** 118
[18] Arndt A, Spoddig D, Esquinazi P, Barzola-Quiquia J, Dusari S and Butz T 2009 *Phys. Rev.* B **80** 195402